

# A novel model for photovoltaic array performance prediction

Wei Zhou <sup>a,\*</sup>, Hongxing Yang <sup>a</sup>, Zhaohong Fang <sup>b</sup>

<sup>a</sup> *Department of Building Services Engineering, The Hong Kong Polytechnic University,  
Hung Hom, Kowloon, Hong Kong*

<sup>b</sup> *School of Thermal Engineering, Shandong University of Architecture, Jinan, Shandong, China*

Received 26 October 2006; received in revised form 20 April 2007; accepted 21 April 2007

---

## Abstract

Based on the  $I$ – $V$  curves of a photovoltaic (PV) module, a novel and simple model is proposed in this paper to predict the PV module performance for engineering applications. Five parameters are introduced in this model to account for the complex dependence of the PV module performance upon solar-irradiance intensity and PV module temperature. Accordingly, the most important parameters, i.e. the short-circuit current, open-circuit voltage, fill factor and maximum power-output of the PV module, may be determined under different solar irradiance intensities and module temperatures. To validate the developed model, field measured data from one existing building-integrated photovoltaic system (BIPV) in Hong Kong was studied, and good agreements between the simulated results and the field data are found. This model is simple and especially useful for engineers to calculate the actual performances of the PV modules under operating conditions, with limited data provided by the PV module manufacturers needed.

© 2007 Elsevier Ltd. All rights reserved.

**Keywords:** PV module;  $I$ – $V$  curve; Short-circuit current; Open-circuit voltage; Fill factor; Maximum power output

---

---

\* Corresponding author. Tel.: +852 2766 4559; fax: +852 2774 6146.  
E-mail address: [w.zhou@polyu.edu.hk](mailto:w.zhou@polyu.edu.hk) (W. Zhou).

### Nomenclature

FF	fill factor of the PV module
$G$	solar irradiance ( $\text{W/m}^2$ )
$K$	Boltzmann constant ( $1.38 \times 10^{-23} \text{ J/K}$ )
$n$	ideality factor of the PV module
$q$	magnitude of the electron charge ( $1.6 \times 10^{-19} \text{ C}$ )
$R_s$	series resistance of the PV module ( $\Omega$ )
$R^2$	coefficient of determination
$T$	PV module temperature (K)
$V_t$	thermal voltage (V)
$v_{oc}$	normalized value of the open-circuit voltage $V_{oc}$ with respect to the thermal voltage $V_t$
$\alpha, \beta, \gamma$	constant parameters for PV module

### Subscripts

A	PV array
M	PV module
MPP	maximum power point
OC	open-circuit
SC	short-circuit

## 1. Introduction

Public awareness of the need to reduce global warming and the drastic increases in oil prices have encouraged many countries around the world to adopt new energy-policies that promote renewable energy applications to meet energy demands and to protect the environment. This is true in both the developed and the developing countries. Solar energy can be mainly utilized in two ways, i.e., either to use it directly for heating or cooling of air and water without using an intermediate electric circuitry, or to convert it into electrical energy by using photovoltaic (PV) modules. Direct conversion of solar radiation into electrical energy is the most convenient way of utilizing solar energy. The advantages of using the photovoltaic effect to generate electricity include no production of pollutants during operation, silent, long lifetime and low maintenance. Moreover, solar energy is abundant, free, clean and inexhaustible.

The performance of a PV module strongly depends on the availability of solar irradiance at the required location and the PV-module temperature. Thus, reliable knowledge and understanding of the PV module performance under different operating conditions is of great importance for correct product selection and accurate prediction of their energy performance.

A lot of work has been done on analysis of the environmental factors that influence PV module performance [1–4]. Kerr and Cuevas [1] presented a new technique, which can determine the current–voltage ( $I$ – $V$ ) characteristics of PV modules based on simultaneously measuring the open-circuit voltage  $V_{oc}$  as a function of a slowly varying light intensity. Others [2–4] generally analyzed the effect of temperature on the performance of PV modules.

There are also some power efficiency models [5–9], which can predict the real dynamic or average performance of a PV system under variable climatic-conditions. No general consensus, however, has been reached on which particular model should be used. Additionally, most of the models have complicated structures, which do not lead themselves to easy manipulation of the system performance; and some detailed parameters, which are normally unavailable in practice, are usually required in the models. Therefore, a simple model with acceptable precision is desirable for PV module performance prediction. The objective of this paper is to pursue a simplified simulation model with acceptable precision to estimate the actual performance of the PV modules under varying operating conditions, with no extra detailed data needed and no complex iteration involved in the calculation.

## 2. Performance prediction model

The four most important electrical characteristics of a PV module are the short-circuit current  $I_{sc}$ , open-circuit voltage  $V_{oc}$ , the fill factor FF and the maximum power output  $P_{max}$  as functions of the solar irradiance intensity and the PV-module temperature. They are modelled as follows.

### 2.1. Short-circuit current $I_{sc}$

At normal levels of solar irradiance, the short-circuit current can be considered equivalent to the photocurrent  $I_{ph}$ , i.e. proportional to the solar irradiance  $G$  ( $\text{W}/\text{m}^2$ ). But this may result in some deviation from the experimental result, so a power law having exponent  $\alpha$  is introduced in this paper to account for the non-linear effect that the photocurrent depends on. The short-circuit current  $I_{sc}$  of the PV modules is not strongly temperature-dependent. It tends to increase slightly with increase of the module temperature. For the purposes of PV module performance, modelling this variation can be considered negligible. Then, the short-circuit current  $I_{sc}$  can be simply calculated by

$$I_{sc} = I_{sc0} \left( \frac{G}{G_0} \right)^\alpha, \quad (1)$$

where  $I_{sc0}$  is the short-circuit current of the PV module under the standard solar irradiance  $G_0$ ; while  $I_{sc}$  is the short-circuit current of the PV module under the solar irradiance  $G$ ;  $\alpha$  is the exponent responsible for all the non-linear effects that the photocurrent depends on.

### 2.2. Open-circuit voltage $V_{oc}$

The relationship of the open-circuit voltage to irradiance is known to follow a logarithmic function based on an ideal diode equation, and the effect of temperature is due to the exponential increase in the saturation current with an increase in temperature [10]. This conclusion causes some difficulties in replicating the observed behaviours of the tested PV modules. Additional terms or some amendatory parameters must be introduced to account for the shunt resistance, series resistance and the non-ideality of the diode. Based on the model given by Van Dyk [11] and then take into account the effect of temperature, the open-circuit voltage  $V_{oc}$  at any given conditions can be expressed by

$$V_{oc} = \frac{V_{oc0}}{1 + \beta \ln \frac{G_0}{G}} \cdot \left( \frac{T_0}{T} \right)^\gamma, \quad (2)$$

where  $V_{oc}$  and  $V_{oc0}$  are the open-circuit voltage of the PV module under the normal solar irradiance  $G$  and the standard solar irradiance  $G_0$ ;  $\beta$  is a PV module technology specific-related dimensionless coefficient [11]; and  $\gamma$  is the exponent considering all the non-linear temperature–voltage effects.

### 2.3. Fill factor $FF$

This is dimensionless; it is a measure of the deviation of the real  $I$ – $V$  characteristic from the ideal one. PV modules generally have a parasitic series and shunt resistance associated with them. Both types of parasitic resistances act to reduce the fill factor. For the PV module with arbitrary values of resistances, a satisfactory empirical expression for the relationship is [12]

$$FF = FF_0 \left( 1 - \frac{R_s}{V_{oc}/I_{sc}} \right), \quad (3)$$

$$FF_0 = \frac{v_{oc} - \ln(v_{oc} + 0.72)}{1 + v_{oc}}, \quad (4)$$

where  $FF_0$  is the fill factor of the ideal PV module without resistive effects;  $R_s$  is the series resistance;  $v_{oc}$  is the normalized value of the open-circuit voltage to the thermal voltage, i.e.

$$v_{oc} = \frac{V_{oc}}{nKT/q}, \quad (5)$$

where  $n$  is the ideality factor ( $1 < n < 2$ );  $K$  is the Boltzmann constant ( $1.38 \times 10^{-23}$  J/K);  $T$  is the PV module temperature (K);  $q$  is the magnitude of the electron charge ( $1.6 \times 10^{-19}$  C).

### 2.4. Maximum power-output $P_{max}$

Making use of the definition of the fill factor, the maximum power output  $P$  delivered by the PV module can be written as

$$\begin{aligned} P_{max} &= FF \cdot V_{oc} \cdot I_{sc} \\ &= \frac{v_{oc} - \ln(v_{oc} + 0.72)}{1 + v_{oc}} \cdot \left( 1 - \frac{R_s}{V_{oc}/I_{sc}} \right) \cdot \frac{V_{oc0}}{1 + \beta \ln \frac{G_0}{G}} \cdot \left( \frac{T_0}{T} \right)^\gamma \cdot I_{sc0} \left( \frac{G}{G_0} \right)^\alpha. \end{aligned} \quad (6)$$

### 2.5. PV array

PV modules represent the fundamental power conversion unit of a photovoltaic system, but a single PV module has limited potential to provide power at high voltage or high current levels. It is then mandatory to connect PV modules in series and in parallel in order to scale-up the voltage and current respectively to tailor the PV array output. If a matrix of  $N_s \times N_p$  PV modules is considered, the scaling rules of voltage and current are as below:

$$I_A = N_p I_M, \quad (7)$$

$$V_A = N_s V_M, \quad (8)$$

where  $I_A$  and  $V_A$  are the PV array current and voltage;  $I_M$  and  $V_M$  are the PV module current and voltage.

We also assume that the fill factor of a PV array, composed of a string of identical PV modules, equals that of a single PV module. The maximum power output of the PV array can be calculated by

$$P_A = FF_A V_A I_A = N_p \cdot N_s \cdot P_M, \quad (9)$$

where  $P_A$  and  $P_M$  are the PV array and PV module power, respectively.

### 3. Model parameter estimation

To carry out the simulation, the five parameters ( $\alpha$ ,  $\beta$ ,  $\gamma$ ,  $R_s$  and  $n$ ) in the model need to be determined first. Beside the data from the specification sheet, a limited number of basic test data are needed, i.e.  $I_{sc}$ ,  $V_{oc}$ , maximum power point current  $I_{MPP}$  and voltage  $V_{MPP}$  of the PV module under two different solar irradiance intensities ( $G_0$ ,  $G_1$ ) and two PV module temperatures ( $T_0$ ,  $T_1$ ) must be used to find the five parameters. The detailed data used for the parameter evaluation are listed in Table 1. To get the required data, one random selected mono-crystalline silicon PV module is tested as a case study.

#### 3.1. Experiment description

The test set-up is shown in Fig. 1. A solar simulator with a 3-phase lamp array is employed to imitate the necessary solar irradiation in the photovoltaic tests. The light source ( $2\text{ m} \times 2\text{ m}$ ) is based on a proven steady-state Halogen Dichroic system, which is made of  $363 \times 75\text{ W}$  lamps powered by 12VDC. The standard steady-state solar simulator can simulate the sunlight in a variety of conditions, with an irradiance from zero to approximately  $1600\text{ W/m}^2$ . As the number of the lamps is large and the diffuse angle of the light is high, the solar-radiation flux on the PV module is uniform.

There are mainly six parameters to be measured in this test, namely the incident solar-irradiance  $G$ , PV module temperature  $T$ , short-circuit current  $I_{sc}$ , open-circuit voltage  $V_{oc}$ , maximum power point current  $I_{MPP}$  and voltage  $V_{MPP}$ . The solar irradiance on the plane of the PV module was monitored with a MS-802 type high-precision pyranometer, which is sensitive in the wavelength range from 305 nm to 2800 nm. The module temperature was measured using a thermocouple which was laminated on the back-surface of the PV module using a conductive paste to ensure good thermal contact. The tested PV module temperature is controlled by the HAAKE Phoenix II refrigerated circulator bath which can maintain the module temperature stable at any point between 20 and 70 °C. The PV module output parameters were measured in the form of  $I$ – $V$  characteristics with a MP-160  $I$ – $V$  curve tracer, which is connected to a personal computer, and the output data were collected by a data logger.

Table 1  
Detailed data requirements for parameter estimation procedures

	$G_0$	$G_1$
$T_0$	$I_{sc}$ , $V_{oc}$ , $I_m$ , $V_m$	$I_{sc}$ , $V_{oc}$ , $I_m$ , $V_m$
$T_1$	Nil	$V_{oc}$

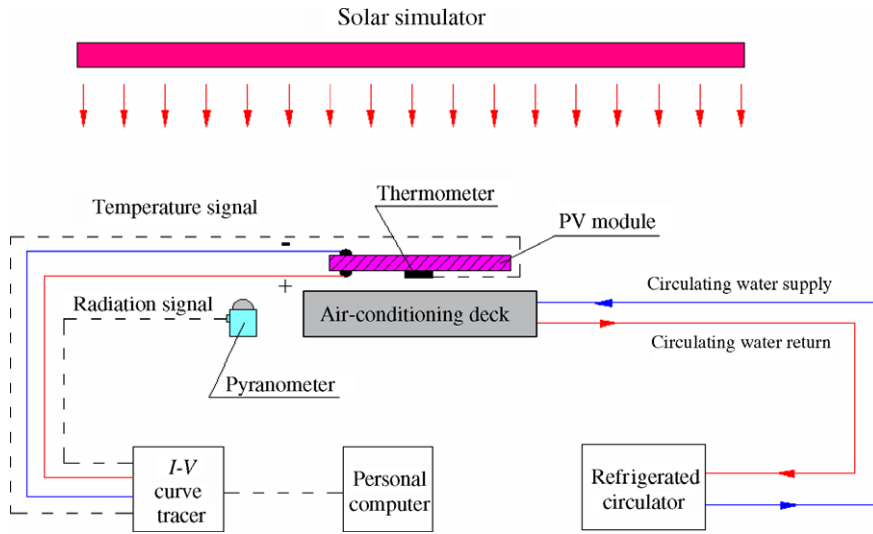


Fig. 1. Diagram of the PV module performance test.

To get the actual performance of the PV module under different solar-irradiance intensities and PV module temperatures, the solar-irradiance intensity of the solar simulator is held invariant at  $G_0 = 1000 \text{ W/m}^2$  and  $G_1 = 400 \text{ W/m}^2$ . Under each intensity, the temperature of the PV module can be adjusted by the HAAKE Phoenix II refrigerated circulator bath system, when the desired temperature  $T_0$  (25 °C) and  $T_1$  (55 °C) is steady, the  $I$ – $V$  curve of the PV module together with other output parameters such as  $I_{sc}$ ,  $V_{oc}$ ,  $I_{MPP}$ ,  $V_{MPP}$ , and  $P_{max}$  can be recorded by the  $I$ – $V$  curve recorded nearly at the same time.

### 3.2. Parameter-estimation procedures

With the available experimental data required in Table 1, the five parameters can be determined one after another by the following procedures:

#### (a) Calculation of the parameter $\alpha$

According to Eq. (1), under different solar-irradiance levels, the short-circuit current  $I_{sc}$  is different, so that the parameter  $\alpha$  can be determined by

$$\alpha = \frac{\ln(I_{sc0}/I_{sc1})}{\ln(G_0/G_1)}, \quad (10)$$

where  $I_{sc0}$  and  $I_{sc1}$  are the short-circuit currents of the PV module under radiation intensity  $G_0$  and  $G_1$ .

#### (b) Calculation of the parameter $\beta$

According to Eq. (2), the open-circuit voltage  $V_{oc}$  varies with both the PV module temperature and the solar irradiance. In order to calculate the parameter  $\beta$ , the PV module temperature is assumed to be constant, and the solar irradiance changes from  $G_0$  to  $G_1$ , and then the parameter  $\beta$  can be calculated by

$$\beta = \frac{V_{oc0}/V_{oc1} - 1}{\ln(G_0/G_1)}, \quad (11)$$

where  $V_{oc0}$  and  $V_{oc1}$  are the open-circuit voltage of the PV module under the solar irradiance of  $G_0$  and  $G_1$  while the PV module temperature remains to be  $T_0$ .

(c) *Calculation of the parameter  $\gamma$*

Similar to the method used in the parameter  $\beta$  calculation, the solar irradiance remains stable, while the PV module temperature changes from  $T_0$  to  $T_1$ , and then the parameter  $\gamma$  can be estimated according to Eq. (2) by

$$\gamma = \frac{\ln(V_{oc0}/V_{oc1})}{\ln(T_1/T_0)}, \quad (12)$$

where  $V_{oc0}$  and  $V_{oc1}$  are the open-circuit voltages of the PV module under two different temperatures  $T_0$  and  $T_1$  when the solar irradiance is at  $G_0$ .

(d) *Calculation of the series resistance  $R_s$*

The series resistance has a significant effect on the performance of a PV module. An accurate knowledge of the series-resistance value is important particularly in computer modelling of PV modules behaviour.

The method of Jia and Anderson [13], based on the one-diode model, supposes the ideality factor  $n$ , variable along the  $I$ – $V$  characteristic of the PV module under illumination with an infinite shunt-resistance  $R_{sh}$  value, is employed in the series-resistance calculations. This method can determine the PV module series-resistance without requiring more information about the module characteristics beyond the data  $V_{oc}$ ,  $I_{sc}$ ,  $V_{MPP}$  and  $I_{MPP}$ , and no complicated testing steps or calculations are involved

$$R_s = \frac{V_{MPP}}{I_{MPP}} \cdot \frac{\frac{1}{V_t} \cdot (I_{sc} - I_{MPP}) \cdot \left[ V_{oc} + V_t \ln \left( 1 - \frac{I_{MPP}}{I_{sc}} \right) \right] - I_{MPP}}{\frac{1}{V_t} \cdot (I_{sc} - I_{MPP}) \cdot \left[ V_{oc} + V_t \ln \left( 1 - \frac{I_{MPP}}{I_{sc}} \right) \right] + I_{MPP}}, \quad (13)$$

where  $R_s$  is the series resistance,  $V_{MPP}$  is the PV module voltage at the maximum power point,  $I_{MPP}$  is the PV module current at the maximum-power point, and  $V_t = kT/q$  is the thermal voltage.

(e) *Calculation of the ideality factor  $n_{MPP}$  at the maximum-power point*

The assumption of a constant diode ideality factor along the entire  $I$ – $V$  output characteristic is commonly used [14], but this assumption is inaccurate at normal intensities and can lead to erroneous results [15].

The PV systems are usually equipped with a maximum-power point tracker to maximize the power output, so that it is reasonable to believe that the PV module working states will stay around the maximum-power point. Therefore, we can simply use the ideality factor at the maximum-power point, which can be determined by the method of Jia and Anderson [13] as long as the series resistance  $R_s$  is known, instead of a constant ideality factor assumption to continue the simulation calculation

$$n_{MPP} = (V_{MPP} + I_{MPP}R_s) / \left[ V_{oc} + V_t \ln \left( \frac{I_{sc} - I_{MPP}}{I_{sc}} \right) \right], \quad (14)$$

where  $n_{MPP}$  is the ideality factor at the maximum-power point.

Following the above procedures, these five parameters ( $\alpha$ ,  $\beta$ ,  $\gamma$ ,  $R_s$  and  $n_{MPP}$ ) can be calculated following the parameter estimation procedures given above, and the results are shown in Table 2.

Table 2

Parameter estimations for the PV modules

$\alpha$	$\beta$	$\gamma$	$n_{\text{MPP}}$	$R_s$ ( $\Omega$ )
1.21	0.058	1.15	1.17	0.012

#### 4. Validation analysis of the simulation model

In this section, the simulation model of the PV array output is verified with measured data for the building-integrated photovoltaic system (BIPV) (on the Hong Kong Polytechnic University campus) which has been working successfully since the year 2000 [16]. The BIPV power-generation system was installed on the three walls and the roof of a plant room on a building and is shown in Fig. 2. The actual grid-connected BIPV system consists of 77 PV modules (the same type of PV module as the one tested above) each of 80 W and a TCG4000/6 inverter, in which 14 modules face east, 21 south, 14 west and 28 on the top. To simplify the validation process, only the 28 PV-modules, which are mounted on the roof with an inclination angle of 22.5°, is employed in the calculation.

The parameters required for the calculation of the system power output were the time series PV-module temperature and horizontal irradiance (the horizontal irradiance will be transformed to the irradiance on the PV-module surface by Duffie and Beckman's model [17]); the measured PV-module temperature and DC array power output were required for the verification of the simulation model. These data were collected every five minutes.

The verification was carried out for two states: sunny conditions and cloudy conditions. Under each section, the simulation model was verified using data from all four seasons. This ensured that the model was verified across the full range of meteorological conditions. At least 1200 sets of values for each of the sunny and cloudy conditions were selected to verify the power-output simulations.

##### 4.1. Sunny conditions model-verification

Calculations of the PV system power output were made for a range of different climatic conditions by compiling data sets for all periods of the year. Four typical days' data sets were compiled according to the season: March, June, September and December. The



Fig. 2. The first grid-connected building-integrated photovoltaic system in Hong Kong.



scatter plots of the calculated power with the measured array output for each of the data periods are compared in Fig. 3.

No strong seasonal effects on the model performance were anticipated, and also it is clearly shown that the calculated sets vary near linearly with the measured curves, and only slight differences were observed. The measurement uncertainty for the calculated values was found to increase with increasing power output in a range from 0 to 200 W. This mismatch was supposed to be mainly caused by the prediction error of the module temperature, which was measured using a thermocouple laminated on the back-surface of the PV module using a conductive paste to ensure good thermal-contact. Because of the convective effect of the surrounding air and the thermal inertia of thermocouple, the thermocouple tends to give a slightly delayed temperature values. Another additional effect was noted to have negative effects on the model performance, i.e. the non-ideal operation of the maximum-power point tracker in the tracking mode.

To present the comparison more clearly, Fig. 4 shows the measured and calculated system power-output profiles for a typical summer day. The simulated power-outputs are found to follow the trend of the measured values quite well.

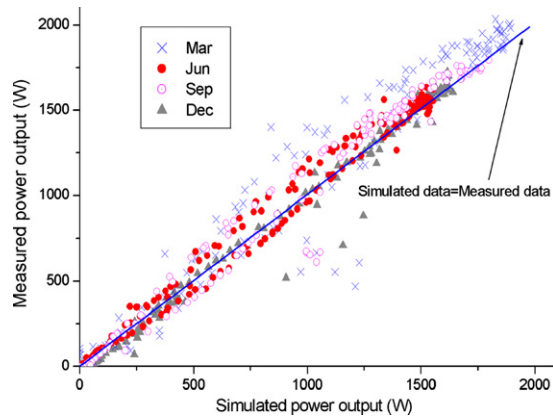


Fig. 3. Correlation between the measured and simulated power-data (Sunny conditions).

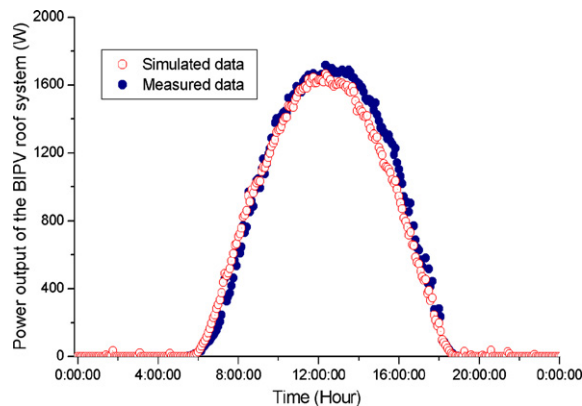


Fig. 4. Comparison between the measured and simulated power-output for a typical sunny summer-day.

4.2. Cloudy-conditions model-verification

The data sets used for cloudy-condition verifications were selected from the same months as for the sunny-day analysis. Fig. 5 shows comparisons against the measured array output for typical days. The measurement uncertainty for the simulated values under cloudy conditions was also found to increase with increasing power output over a range from 0 to 250 W. With the range of measurement uncertainty taken into consideration, the differences of the output for different seasons and different temperature conditions were found to be small.

Fig. 6 shows the power-output comparison profiles for the typical summer day for the cloudy conditions, and the predicted power output was found to track the measured variations quite well.

To evaluate how well a simulation model has captured the variation of the field data, and to assess the simulation model performance when different data sets are used, the coefficient of determination  $R^2$  is employed, where

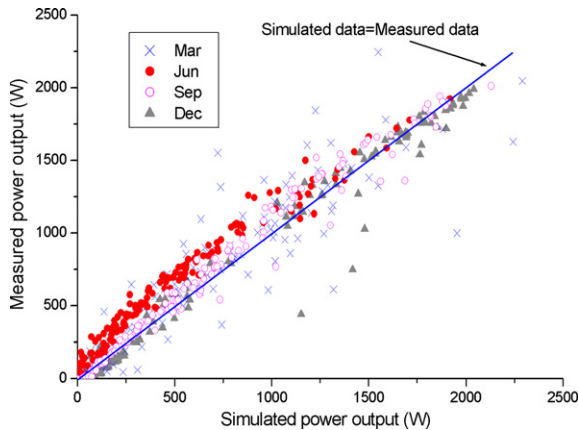


Fig. 5. Correlation between the measured and simulated power-data (Cloudy conditions).

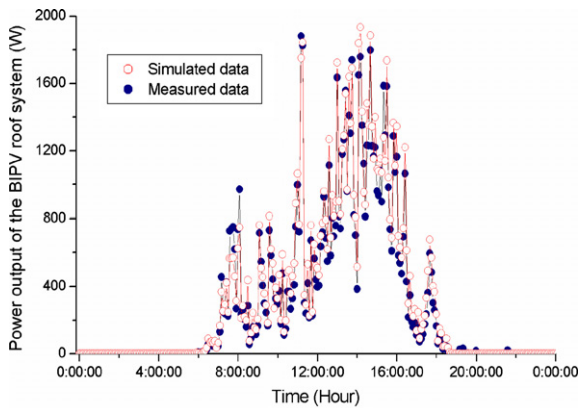


Fig. 6. Comparison between the measured and simulated power-output for a typical cloudy summer-day.

$$R^2 = 1 - \frac{\sum (y_i - \hat{y}_i)^2}{\sum (y_i - \bar{y})^2}, \quad (15)$$

and  $y_i$  is the field measured data,  $\bar{y}$  is the arithmetic mean of the field data, and  $\hat{y}_i$  is the simulation model predicted value. The higher the value of  $R^2$  the stronger the linear correlation between the calculated power and the measured power, i.e. the better the simulation performance.

The coefficient of determination  $R^2$  for the studied cloudy-conditions is found to be 0.96; it is a little lower than 0.98 for the sunny conditions. Bigger measurement error of the module temperature under cloudy conditions than under sunny conditions are supposed to be the reason. Generally speaking, under cloudy conditions, due to the rapidly changing irradiance caused by the passing clouds over the sun, the PV module temperature changes quickly, up and down, before it is fully recorded by the thermocouple which is laminated on the back-surface of the PV module. Anyway, these two high coefficients of determination  $R^2$  for these two studied conditions demonstrated the good prediction performance of the simulation model.

## 5. Conclusions

The performance of the PV module is highly influenced by the weather, especially the solar irradiance and the PV-module temperature. In this paper, a simple parameter-estimation-based model is presented for the PV-module performance calculations. Five parameters ( $\alpha$ ,  $\beta$ ,  $\gamma$ ,  $R_s$  and  $n_{MPP}$ ) are introduced to take account of all the non-linear effect of the environmental factors on the PV module performance, and the parameters' calculation procedures are clearly given. Other than a consistent assumption of the fill factor, it is calculated by the ideality factor  $n_{MPP}$  at the maximum-power point and the series resistance  $R_s$ . It also employs module parameters that are more likely to be available on manufacturers' data sheets.

The model's accuracy is demonstrated by comparing the predictions with the field measured data. To ensure the model was verified across the full range of meteorological conditions, the verification was carried out for two states: sunny conditions and cloudy conditions. Under each section, the simulation model was verified using data for all four seasons. The results demonstrate an acceptable accuracy of the model for modelling PV array outputs under various environmental conditions.

## References

- [1] Kerr MJ, Cuevas A. Generalized analysis of the illumination intensity vs. open-circuit voltage of PV modules. *Sol Energy* 2003;76:263–7.
- [2] Radziemski E, Klugmann E. Thermally-affected parameters of the current–voltage characteristics of silicon photocell. *Energ Convers Manage* 2002;43:1889–900.
- [3] Van Dyk EE et al. Temperature-dependent of performance of crystalline silicon photovoltaic modules. *S Afr J Sci* 2000;96:198–200.
- [4] Nishioka K et al. Field-test analysis of PV-system-output characteristics focusing on module temperature. *Sol Energy Mater PV module* 2003;75:665–71.
- [5] Evans DL. Simplified method for predicting photovoltaic array output. *Sol Energy* 1981;27:555–60.

- [6] Mondol JD, Yohanis YG, Smyth M, Norton B. Long-term validated simulation of a building integrated photovoltaic system. *Sol Energy* 2005;78:163–76.
- [7] Hove T. A method for predicting long-term average performance of photovoltaic systems. *Renew Energ* 2000;21:207–29.
- [8] Stamenic L, Smiley E, Karim K. Low light conditions modelling for building integrated photovoltaic (BIPV) systems. *Sol Energy* 2004;77:37–45.
- [9] Jones AD, Underwood CP. A modelling method for building-integrated photovoltaic power supply. *Building Serv Eng Tes Technol* 2002;23:167–77.
- [10] Luis C, Sivestre S. Modelling photovoltaic systems using PSpice. Chichester: John Wiley & Sons Ltd.; 2002.
- [11] Van Dyk EE et al. Long-term monitoring of photovoltaic devices. *Renew Energ* 2002;22:183–97.
- [12] Green MA. PV modules: operating principles, technology and system applications. Sydney: UNSW; 1992.
- [13] Jia QZ, Anderson WA. A novel approach for evaluating the series resistance of solar cells. *Sol cells* 1988;25:311–8.
- [14] Bashahu M, Habyarimana A. Review and test of methods for the determination of the PV module series resistance. *Renew Energ* 1995;6:129–38.
- [15] Hamdy MA, Cell RL. The effect of the diode-ideality factor on the experimental determination of series resistance of solar cells. *Sol cells* 1987;20:119–26.
- [16] Yang HX et al. Grid-connected building-integrated photovoltaics: a Hong Kong case study. *Sol energy* 2004;76:55–9.
- [17] Duffie JA, Beckman WA. Solar engineering of thermal processes. USA: John Wiley & Sons; 1980.